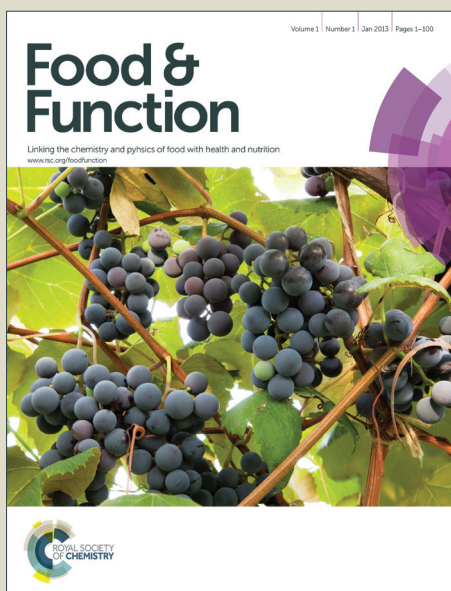


# Food & Function

Accepted Manuscript



This is an *Accepted Manuscript*, which has been through the Royal Society of Chemistry peer review process and has been accepted for publication.

*Accepted Manuscripts* are published online shortly after acceptance, before technical editing, formatting and proof reading. Using this free service, authors can make their results available to the community, in citable form, before we publish the edited article. We will replace this *Accepted Manuscript* with the edited and formatted *Advance Article* as soon as it is available.

You can find more information about *Accepted Manuscripts* in the [Information for Authors](#).

Please note that technical editing may introduce minor changes to the text and/or graphics, which may alter content. The journal's standard [Terms & Conditions](#) and the [Ethical guidelines](#) still apply. In no event shall the Royal Society of Chemistry be held responsible for any errors or omissions in this *Accepted Manuscript* or any consequences arising from the use of any information it contains.

1     **Structural Characterization and Immunomodulatory Activity of**  
2             **a New Heteropolysaccharide from *Prunella vulgaris***

3  
4     Chao Li<sup>a,b</sup>, Lijun You<sup>a</sup>, Xiong Fu<sup>a,\*</sup>, Qiang Huang<sup>a,\*</sup>, Shujuan Yu<sup>a</sup>, Rui Hai Liu<sup>a,c</sup>

5  
6     <sup>a</sup> College of Light Industry and Food Science, South China University of Technology,  
7     381 Wushan Road, Guangzhou 510640, China

8     <sup>b</sup> Department of Food Science, Rutgers University, 65 Dudley Road, New Brunswick,  
9     NJ 08901, USA

10    <sup>c</sup> Department of Food Science, Stocking Hall, Cornell University, Ithaca, NY, 14853,  
11    USA

12  
13  
14    \* Co-corresponding authors

15    **Xiong Fu**, Telephone: +86 20 87113668; fax: +86 20 87113668; E-mail:  
16    lxfu@scut.edu.cn;

17    **Qiang Huang**, Telephone: +86 20 87113845; fax: +86 20 87113848; E-mail:  
18    fechoh@scut.edu.cn

19 **Abstract**

20 A new heteropolysaccharide, here called P1, was isolated from the fruit clusters of *Prunella*  
21 *vulgaris* using hot water extraction method. Chemical and physical analyses indicated that P1  
22 had a spherical conformation with an average molecular weight of 1,750 kDa, and consisted of  
23 arabinose (28.37%), xylose (54.67%), mannose (5.61%), glucose (5.46%), and galactose  
24 (5.89%). The main linkage types of P1 were proved to be (1→5)-linked  $\alpha$ -L-Ara, (1→)-linked  
25  $\alpha$ -L-Ara, (1→3)-linked  $\alpha$ -D-xyl, (1→3)-linked  $\beta$ -D-Gal, (1→3,6)-linked  $\beta$ -D-Gal,  
26 (1→3,6)-linked  $\alpha$ -D-Man and (1→6)-linked  $\alpha$ -D-Glc according to periodate oxidation-Smith  
27 degradation and NMR analyses. P1 could significantly enhance the secretion of NO, TNF- $\alpha$ ,  
28 and IL-6 in murine RAW 264.7 cells involving the toll-like receptor 2 (TLR2), TLR4 and  
29 complement receptor 3 (CR3). Further studies showed that P1 exhibited stable immune  
30 activities in the pH range of 4.0-10.0 and below 121 °C. The results suggested that P1 could be  
31 used as a potent immunomodulatory agent in functional foods and pharmacological fields.

32 **Key words:** polysaccharide, *Prunella vulgaris*, structural characterization, immunomodulatory,  
33 toll-like receptor

## 34 1. Introduction

35 Macrophages, a kind of innate immune cells, are involved in many processes, such as tissue  
36 remodeling during embryogenesis, wound repair, clearance of apoptotic cells, hematopoiesis,  
37 and homeostasis. They also play pivotal roles in the defense against microbial invasion and  
38 tumorigenesis.<sup>1,2</sup> Therefore, macrophages are usually chosen as ideal cell models to examine  
39 the immune-modulating effects of bioactive compounds. The role of activated macrophages in  
40 the immune system involves the release of various inflammatory mediators and cytokines, such  
41 as nitric oxide (NO), tumor necrosis factor (TNF), interleukin (IL), and reactive oxygen species  
42 (ROS).<sup>3</sup> Activation of macrophages required activation signals to trigger cytokine synthesis and  
43 release.<sup>4</sup> Development of polysaccharides to augment innate immune responses has attracted  
44 much attention during the past several decades.

45 Polysaccharides, considered as biological response modifiers (BRMs), show a number of  
46 beneficial therapeutic properties. They are widely used as potent immunotherapeutic agents  
47 with no serious side effects.<sup>5,6</sup> The primary effect of polysaccharides is to enhance and/or  
48 activate macrophages immune responses through membrane receptors, resulting in  
49 immunomodulation, anti-tumor activity, wound-healing and other therapeutic effects.<sup>3</sup> Glucans  
50 are an important type of polysaccharides and their bioactivities are highly dependent on their  
51 structural characteristics, including molecular weight, monosaccharide composition, backbone  
52 linkage, degrees of branching, and branch linkage. The  $\beta$ -glucan with a 1 $\rightarrow$ 3 and 1 $\rightarrow$ 6 linked  
53 main chain shows antitumor and immunomodulatory activities, while  $\alpha$ -glucan with 1 $\rightarrow$ 4  
54 linked main chain usually serves as food nutrients. For example, polysaccharides isolated from  
55 mushrooms are typical  $\beta$ -glucans, showing strong antitumor and immunomodulatory activities.<sup>7,</sup>  
56 <sup>8</sup> Therefore, it is important to search new polysaccharides with unique structure and high

57 immunity activity as novel BRMs.

58 *Prunella vulgaris* L., which belongs to the family of Lamiaceae, is a medicine food  
59 homology plant widely cultivated in China and Europe. The fruit clusters of *P. vulgaris* have  
60 long been used as a traditional medicine to alleviate sore throat, reduce fever and accelerate  
61 wound healing in folk.<sup>9</sup> In China, it has been extensively used as a health-promoting food and  
62 traditional Chinese medicine (TCM) for treatment of hypertension, jaundice, hepatitis,  
63 tuberculosis, mammitis, diabetes mellitus, *etc.*<sup>10</sup> To date, some polysaccharides isolated from  
64 the fruit clusters of *P. vulgaris* have been demonstrated to have antioxidant, antiproliferative  
65 and immune-stimulatory effects.<sup>11-13</sup> However, little work has been reported on the structural  
66 characterization, biological function and mechanisms of the immunomodulatory activities of  
67 the polysaccharides from *P. vulgaris*.

68 In the present study, a new heteropolysaccharide, named P1, was extracted from *P. vulgaris*  
69 using hot water extraction. The primary structures and conformation of P1 were characterized  
70 and its immunomodulatory activities and immune receptors using murine macrophage RAW  
71 264.7 cells were investigated. In addition, the stability of P1 bioactivity under different pH  
72 values and thermal treatments were investigated. The results will provide significant  
73 information for the application of this plant in functional foods and pharmacological fields in  
74 the future.

## 75 **2. Materials and Methods**

### 76 *2.1. Materials and Chemicals*

77 The fruit clusters of *P. vulgaris*, derived from Hubei province of China, were purchased from  
78 Qingping medicinal material market (Guangzhou, China). The murine macrophage RAW 246.7

79 cell line was obtained from American Type Culture Collection (ATCC, Rockville, MD, USA).  
80 Dulbecco's modified eagle medium (DMEM), penicillin-streptomycin and phosphate-buffered  
81 saline (PBS, pH 7.4) were purchased from Gibco Life Technologies (Grand Island, NY, USA).  
82 Fetal bovine serum (FBS) was purchased from Zhejiang Tianhang Biological Technology Co.  
83 (Zhejiang, China). Anti-TLR2 antibody, anti-TLR4 antibody and Anti-CR3 antibody were  
84 purchased from Abcam Inc. (Cambridge, MA). Laminarin (Lam), lipopolysaccharide (LPS,  
85 isolated from *E. coli* strain 055: B5) were purchased from Sigma-Aldrich Chemical Co. (St. Louis,  
86 MO, USA). Standards of dextran and monosaccharides, uronic acid, glycol, glycerol, and  
87 erythritol were purchased from Sigma-Aldrich Chemical Co. (St. Louis, MO, USA). DEAE  
88 (diethylaminoethyl)-Sephacrose and Sephadex G-200 were purchased from GE Healthcare Life  
89 Science (Piscataway, NJ, USA). Nitric oxide (NO)-detecting kit was purchased from Nanjing  
90 Jiancheng Institute of Biotechnology (Nanjing, China). The mouse TNF- $\alpha$  enzyme-linked  
91 immunosorbent assay (ELISA) kit and the mouse IL-6 ELISA kit were purchased from  
92 Neobioscience Technology Co., Ltd. (Shenzhen, China). Other chemicals and reagents used in  
93 this study were of analytical grade.

#### 94 *2.2. Extraction, Isolation, and Purification of Polysaccharides*

95 The crude polysaccharides were prepared and then fractionated according to the method  
96 described previously.<sup>13</sup> Three fractions, PV-P1, PV-P2, and PV-P3 were obtained by  
97 freeze-drying. The PV-P1 showed the most pronounced immune ability (data not shown). For  
98 this reason, PV-P1 was further purified by Sephadex G-100 column chromatography. Ten  
99 milligrams of PV-P1 were re-dissolved in 1 mL of distilled water and loaded onto a Sephadex  
100 G-100 column (10 mm  $\times$  400 mm). The sample was eluted with distilled water at a speed of 0.2

101 mL/min. The eluent was collected with an automatic collector and then examined. The elution  
102 curve was drawn using the tube number and absorbance (490 nm). The elution peaks were  
103 evaluated and the P1 fraction (Fig.1A) was collected and then freeze-dried. The carbohydrate  
104 content of P1 was measured by the phenol-sulfuric acid method.<sup>14</sup>

### 105 2.3. Physicochemical Properties

106 Physicochemical properties of P1 were determined by color observation, solubility test, and  
107 iodination reaction. The absorption spectrum of P1 solution was recorded using a TU-1901  
108 UV-vis spectrophotometer (Beijing Purkinje General Instrument Co., Ltd., Beijing, China) in  
109 the wavelength range of 190-800 nm.

### 110 2.4. Determination of Molecular Weight

111 The molecular weight of the purified polysaccharide was measured using gel-permeation  
112 chromatography (GPC) performed on a Waters instrument equipped with the TSK-GEL  
113 columns (Tosoh Co., Ltd, Tokyo, Japan) in series of G5000 PW<sub>XL</sub> (7.8 × 300 mm i.d., 10 μm)  
114 and G3000PW<sub>XL</sub> (7.8 × 300 mm i.d., 5 μm). The mobile phase was 0.02 M KH<sub>2</sub>PO<sub>4</sub> (pH 6.0) at  
115 a flow rate of 0.6 mL/min. The column temperature was kept at 35.0 ± 0.1 °C. The injection  
116 volume was 20 μL in each run. The calibration curve of dextran standards obtained was  
117  $\text{Log}M_w = 36.803 - 5.5527V + 0.3325V^2 - 0.007V^3$  (where  $M_w$  represents the molecular weight, while  
118  $V$  represents elution volume) with a correlation coefficient of 0.9999. The elution volume of P1  
119 was plotted in the same calibration curve, and the molecular weight was determined.

### 120 2.5. Infrared (IR) Spectrum

121 The infrared spectrum was collected using a Vector 33 FT-IR spectrophotometer (Bruker,  
122 Ettlingen, Germany). The P1 was ground with KBr powder and then pressed into pellets for

123 transmission IR measurement in the wavenumber range of 500-4000  $\text{cm}^{-1}$ .<sup>15</sup>

#### 124 *2.6. Uronic Acid Analysis*

125 Galacturonic acid and glucuronic acid contents were measured according to the method  
126 described previously.<sup>8</sup> Briefly, P1 (5 mg) was hydrolyzed in a sealed tube with 2 M trifluoroacetic  
127 acid (4 mL) at 105 °C for 6 h. The residue was re-dissolved in distilled water (10 mL) and  
128 filtered through a 0.22  $\mu\text{m}$  microporous filtering film. The operation was done using a Dionex ion  
129 chromatography ICS 5000 (Sunnyvale, CA, USA) with a CarboPac PA1 analytic column (4  $\times$  250  
130 mm). Galacturonic acid and glucuronic acid were used as standards.

#### 131 *2.7. Monosaccharide Composition Analysis*

132 The monosaccharide composition was determined as previously described.<sup>16</sup> P1 (5 mg) was  
133 hydrolyzed in a sealed tube with 2 M trifluoroacetic acid (4 mL) at 105 °C for 6 h. Excess  
134 trifluoroacetic acid was removed by evaporation under reduced pressure. The residue was  
135 dissolved in methanol and evaporated to dryness for three times. The residue was re-dissolved in  
136 methanol (2 mL), and transferred to a glass tube. The solution was blow-dried with nitrogen.  
137 Hydroxylamine hydrochloride (10 mg), inositol hexacetate (1 mg), and pyridine (2.0 mL) were  
138 added in the tube. The sealed tube was immersed in a thermostatic water bath at  $90 \pm 1$  °C for 30  
139 min. Then, acetic anhydride (2 mL) was added and kept at 90 °C for 30 min. Distilled water (2  
140 mL) was added to terminate the reaction. The acetylated derivatives were extracted with  
141 methylene chloride (4 mL). The methylene chloride layer was treated with anhydrous sodium  
142 sulfate and filtered through a 0.22  $\mu\text{m}$  microporous filtering film. GC was performed on a gas  
143 chromatography/mass spectrometer (Trace DSQ II, Thermo Fisher Scientific, Waltham, MA,  
144 USA) equipped with a TR-5MS capillary column (30 m  $\times$  0.25 mm  $\times$  0.25  $\mu\text{m}$ ). The temperature

145 program was set as follows: the initial temperature of the column was 100 °C and held for 2 min,  
146 then increased to 280 °C at 5 °C/min and held for 5 min. The flow rate was 1 mL/min. The  
147 injection temperature was 250 °C. The ion source of the mass spectrometer was set at 280 °C.  
148 The injection volume was 1 µL and the split ratio was 10:1.

#### 149 *2.8. Periodate Oxidation-Smith Degradation*

150 The periodate oxidation-Smith degradation assay was carried out according to the method  
151 described previously.<sup>8</sup> Briefly, P1 (20 mg) was dissolved in distilled water (12.5 mL), and 30 mM  
152 NaIO<sub>4</sub> (12.5 mL) was then added. The solution was kept in the dark at room temperature until the  
153 optical density value at 223 nm became stable. The oxidation solution (2 mL) was titrated with  
154 NaOH standard solution (0.01 M) to calculate the production of formic acid. The rest was  
155 dialyzed against distilled water, and the residue was reduced with NaBH<sub>4</sub> in the dark for 24 h,  
156 neutralized to pH 6.0-7.0 with 50% acetic acid, dialyzed, and concentrated to dryness. The residue  
157 was hydrolyzed with 2 M trifluoroacetic acid in a sealed glass tube. The residue was dissolved in  
158 methanol and evaporated to dryness for three times. Acetylation was carried out with  
159 hydroxylamine hydrochloride and pyridine in the sealed tube at 90 °C for 30 min. Then, acetic  
160 anhydride (1 mL) was added for another 30 min. The acetate derivate was analyzed using a gas  
161 chromatography (GC) spectrometer. Glycol, glycerol, erythritol, rhamnose, arabinose, xylose,  
162 mannose, glucose, and galactose were used as standards.

#### 163 *2.9. NMR Spectroscopy*

164 NMR analysis was carried out on a Bruker 600 MHz (Bruker Corp., Fallanden, Switzerland).  
165 P1 (30 mg) was dissolved in D<sub>2</sub>O (0.6 mL). <sup>1</sup>H NMR and <sup>13</sup>C NMR spectra were obtained at  
166 25 °C. All chemical shifts were expressed in ppm.

### 167 2.10. Atomic Force Microscopy (AFM)

168 The morphological characteristics of the polysaccharide P1 was observed by Tapping Mode  
169 (TM)-AFM (Nanoscope 3A Multimode, Veeco Co., USA) in air at room temperature with a  
170 relative humidity of 65% according to the method described previously.<sup>17</sup> P1 (1 mg) was  
171 dissolved in distilled water (1.0 mL) with continuous stirring for 2 h in a water bath at 60 °C.  
172 After cooling to room temperature, the solution was diluted to a final concentration of 2.5 µg/mL,  
173 gently stirred overnight and filtered through a 0.45 µm microporous filtering film. Approximately  
174 5 µL of aliquot (2.5 µg/mL) was pipetted onto freshly cleaved surface of mica sheet. After drying  
175 fully in air, the mica sheet was pasted to a round metal plate and then placed on the magnetic  
176 observing platform. The image was examined using TM-AFM with a silicon probe (Tap  
177 150-G-10, Ted Pella, INC., USA) and captured at a scan rate of 1.0 Hz and tip velocity of 600  
178 µm/S. Software *WSxM* (Nanotec Electronica, Spain) was used to process AFM image.

### 179 2.11. Preparation of P1 Solutions for Cell Culture

180 (1) P1 solutions were prepared in culture medium at concentrations of 62.5, 125, 250, and  
181 500 µg/mL. (2) P1 in phosphate buffers (PBS) (6 mL) at a concentration of 2 mg/mL was divided  
182 into three parts and thermal treated for 30 min at 100, 121, and 145 °C, respectively. Then each  
183 part was adjusted to a concentration of 400 µg/mL using culture medium. (3) P1 (2 mg/mL) was  
184 dissolved in PBS to adjust final pH 2.0, 4.0, 6.0, 7.4, 8.0, and 10.0, respectively. All samples were  
185 placed overnight at room temperature and then adjusted to the concentration of 400 µg/mL with  
186 culture medium. All solutions were sterilized using a 0.22 µm microporous filtering film and then  
187 incubated with RAW 264.7 cells.

### 188 2.12. Cell Culture and Sample Treatment

189 RAW 264.7 cells were cultured in DMEM containing 10% FBS, 100  $\mu\text{g}/\text{mL}$  streptomycin  
190 and 100 U/mL penicillin in a humidified incubator with 5%  $\text{CO}_2$  at 37  $^\circ\text{C}$ . Cells in the  
191 logarithmic growth phase were adjusted to the concentration of  $1 \times 10^6$  cells/mL. The cell  
192 solutions (100  $\mu\text{L}$ ) and sterilized PBS (100  $\mu\text{L}$ ) were added to each well. Cells were cultured at  
193 37  $^\circ\text{C}$  in a 5%  $\text{CO}_2$  humidified atmosphere incubator for 24 h. The culture medium was then  
194 refreshed, and cells were incubated with P1 sample. The immune receptors of P1 were  
195 determined by antibody inhibition experiments. The cells were incubated with the monoclonal  
196 antibodies (5  $\mu\text{g}/\text{mL}$ ) and Lam (500  $\mu\text{g}/\text{mL}$ ) for 1 h before stimulation with P1. LPS (50  $\mu\text{g}/\text{mL}$ )  
197 was used as the positive control. The supernatants were collected after 24 h incubation. The  
198 concentrations of NO, TNF- $\alpha$  and IL-6 were determined using the NO-detecting kit, mouse  
199 TNF- $\alpha$  kit and mouse IL-6 ELISA kit, respectively, according to the manufacturer's  
200 instructions.

### 201 *2.13. Statistical Analysis*

202 Data were presented as mean  $\pm$  standard deviation (SD) with triplicates. Significance was  
203 determined at  $p < 0.05$  by one-way analysis of variance followed by Duncan's least significant  
204 using SPSS 13.0 software (SPSS, Inc., Chicago, IL, USA).

## 205 **3. Results and Discussion**

### 206 *3.1. Physicochemical Properties*

207 Polysaccharide P1 exhibited white color and was soluble in water, especially in the hot-water.  
208 It cannot be dissolved in organic solvents such as methanol, ethanol, acetone, ethyl acetate, and  
209 butyl alcohol. The result of the iodination test indicated that P1 did not contain starch. No  
210 ultraviolet absorption peaks at 260 and 280 nm also suggested the absence of nucleic acid and

211 protein in P1. The total carbohydrate content of P1 was determined to be 97.5% (w/w).

### 212 3.2. Chemical Structures

213 The molecular weight distribution of P1 is shown in Fig. 1B. P1 comprised of a  
214 polysaccharide with an average molecular weight of 1,750 kDa. Results of gas chromatography  
215 suggested that P1 was composed of arabinose, xylose, mannose, glucose, and galactose with  
216 molar percentages of 28.37, 54.67, 5.61, 5.46, and 5.89%, respectively (Fig. 3).

217 The IR spectrum of P1 showed the absorption peaks at 3374, 2928, and 1422  $\text{cm}^{-1}$ ,  
218 corresponding to the stretching of the O-H, C-H, and carboxyl C-O groups (Fig. 2A). The  
219 absorption peak at 1605  $\text{cm}^{-1}$  was due to the bound water. The peak in the region of 1249  $\text{cm}^{-1}$   
220 was assigned to O-H deformation vibrations. A characteristic absorption at 901  $\text{cm}^{-1}$  indicated  
221 the presence of  $\beta$  anomeric configurations, while the absorption at 1046  $\text{cm}^{-1}$  was typical for the  
222 pyranose form.<sup>18</sup> A weak characteristic peak at 1745  $\text{cm}^{-1}$  indicated the existence of uronic acid  
223 in the polysaccharide structure.<sup>19</sup> The equation of the standard curve made by different  
224 concentrations of galacturonic acid and the peak area is shown in Fig. 2B. The result of ion  
225 chromatography analysis indicated that the content of galacturonic acid was 2.9% (w/w) (based  
226 on dry weight of P1) (Fig. 2C).

227 Using periodate oxidation, Smith degradation, and gas chromatography (GC), the position of  
228 glycosidic linkages in P1 was measured (Fig. 4). The standard curve of  $\text{NaIO}_4$  is shown in Fig.  
229 4C. According to the equation of standard curve, results of periodate oxidation showed that  
230 0.794 mol of  $\text{HIO}_4$  consumed and 0.350 mol of formic acid produced per hexose residue,  
231 indicating that the (1 $\rightarrow$ )-linked or (1 $\rightarrow$ 6)-linked glycosyl linkages accounted for 35.0% and the  
232 (1 $\rightarrow$ 2)-linked or (1 $\rightarrow$ 4)-linked glycosyl linkages accounted for 9.4% of all linkages in the

233 molecule.<sup>19</sup> The oxidized P1 was converted into the corresponding alditol acetate for GC  
234 analysis. The presence of five monosaccharides revealed that some of the linkages were  
235 (1→3)-linked, (1→2,4)-linked, (1→2,3)-linked, (1→3,4)-linked, or (1→2,3,4)-linked glycosyl  
236 linkages, accounting for about 55.6% of all linkages in the molecule.<sup>20</sup> And these linkages  
237 could not be oxidized. The presence of glycerol and erythritol indicated the presence of the  
238 (1→2)-linked, (1→6)-linked, and/or (1→2,6)-linked, as well as (1→4)-linked and/or  
239 (1→4,6)-linked glycosyl bonds.<sup>21, 22</sup>

240 The spectra of <sup>1</sup>H NMR and <sup>13</sup>C NMR of P1 are shown in Fig. 5. Signals of P1 in <sup>1</sup>H NMR  
241 and <sup>13</sup>C NMR spectra were assigned based on the monosaccharide composition, linkage  
242 analysis, and chemical shifts.<sup>20, 23-26</sup> The <sup>1</sup>H NMR spectrum contained five signals at δ 5.48,  
243 5.28, 5.26, 5.16, and 4.94 ppm for the anomeric protons, indicating five residues designated as  
244 (1→5)-linked α-L-Ara, (1→)-linked α-L-Ara, (1→3,6)-linked α-D-Man, (1→3)-linked α-D-xyl,  
245 and (1→6)-linked α-D-Glc, respectively (Fig. 5A). Signals at δ 4.61, 4.55, 4.53, 4.50 ppm were  
246 assigned to (1→6)-linked β-D-Gal, β-galacturonic acid, (1→3)-linked β-D-Gal, and  
247 (1→3,6)-linked β-D-Gal, respectively. The chemical shifts from δ 3.4 to 4.0 ppm were assigned  
248 to proton signals of carbons C-2 to C-6 of sugar rings.<sup>21</sup> The <sup>13</sup>C NMR spectrum showed seven  
249 signals in the anomeric region (δ 95-110 ppm), which were assigned to α (δ 95-102 ppm) and β  
250 (δ 103-110 ppm) anomeric configuration (Fig. 5B). Signals at δ 95.98, 97.24, 100.19, 101.33,  
251 109.16 ppm were attributed to the anomeric carbon atoms of (1→3,6)-linked α-D-Man,  
252 (1→6)-linked α-D-Glc, (1→3)-linked α-D-xyl, (1→5)-linked α-L-Ara, and (1→)-linked  
253 α-L-Ara units, respectively. The signal at δ 105.99 ppm was due to C-1 of β-galacturonic acid,  
254 (1→3)-linked β-D-Gal, and (1→6)-linked β-D-Gal units. The signals from δ 55.17 to 86.26

255 ppm were assigned to carbons C-2 to C-6 of the residues.<sup>23</sup>

256 Previous chemical analysis results indicated that P1 had different chemical compositions and  
257 structure characteristics.<sup>27, 28</sup> The structural differences might be due to the differences in  
258 extraction methods, the specific *P. vulgaris* strain, and growing conditions. Different analytical  
259 methods may also generate different results.<sup>16, 29</sup>

### 260 3.3. Molecular Morphology

261 AFM can intuitively provide three-dimensional structural information of macromolecules and  
262 is widely used for observing the surface morphology or structure of polymers.<sup>30</sup> AFM image  
263 showed that the morphological chain conformation of the P1 was spherical in distilled water  
264 (Fig. 6). The spherical polysaccharides have the potential of being used in the drug delivery and  
265 controlled release fields.<sup>31, 32</sup>

### 266 3.4. Immunomodulatory activity

#### 267 3.4.1. Effects of Different Concentrations of P1 on Cytokine Production

268 Cytokines, such as NO, TNF- $\alpha$ , and IL-6, secreted from activated macrophages play a pivotal  
269 role in fighting microbial invasion and tumorigenesis. NO, TNF- $\alpha$ , and IL-6 are widely used as  
270 immune response parameters.<sup>33</sup> Our previous study demonstrated that *P. vulgaris*  
271 polysaccharide had no cytotoxicity to RAW 264.7 cells within the tested concentrations in this  
272 study (data not shown). Effects of different concentrations of P1 on NO, TNF- $\alpha$ , and IL-6  
273 production are shown in Fig. 7. NO production is regulated by the expression of inducible oxide  
274 synthase (iNOS) in activated macrophages.<sup>34</sup> The activation of macrophages required activation  
275 signals. Thus, the level of NO in the control was very low. P1 remarkably increased the  
276 secretion levels of NO and IL-6 in RAW 264.7 cells in a dose-dependent manner within the

277 tested concentrations (Fig. 7A, C). P1 also increased the TNF- $\alpha$  production in a dose-dependent  
278 manner below the concentration of 125  $\mu\text{g/mL}$  (Fig. 7B). When the concentration increased  
279 from 125 to 250  $\mu\text{g/mL}$ , the amount of TNF- $\alpha$  remained stable. The result indicated the  
280 existence of maximum dosage for the secretion of TNF- $\alpha$ . Overall, these results confirmed that  
281 P1 had significant immunomodulatory activity. Previous studies demonstrated that the  
282 anti-cancer activity and immunomodulatory activity of polysaccharide were mainly related to  
283 the (1 $\rightarrow$ 3)-D-glucans in its molecular structure.<sup>7, 35, 36</sup> P1 with 55.6% (molar percentage) of  
284 (1 $\rightarrow$ 3)-linked glycosyl linkages may account for its significant immunomodulatory activity.  
285 Furthermore, the triple-helix conformation of (1 $\rightarrow$ 3)-D-glucans played an important role in  
286 influencing cytokine stimulating activity and antitumor activity.<sup>37, 38</sup> Previous studies  
287 demonstrated that some polysaccharides had immunomodulatory activities in the triple-helix  
288 conformation but not as a single flexible chain.<sup>17, 38, 39</sup> However, Xu et al. (2012) found a  
289 polysaccharide lacking triple-helix conformation from *Lentinula edodes* also had  
290 immuno-modulating activities.<sup>40</sup> Our study demonstrated that polysaccharides from *P. vulgaris*  
291 had no triple-helix conformation by Congo red assay (data not shown). AFM showed that P1  
292 had spherical conformation when dispersed in water. Previous studies demonstrated that  
293 polysaccharides with sphere-like conformation had antitumor activity *in vitro*.<sup>41</sup> Thus, the  
294 spherical conformation of polysaccharide would affect its immunomodulatory activity. In-depth  
295 investigations on the relationship between spherical conformation and biological activities of  
296 P1 are underway. These results indicated that P1, a new heteropolysaccharide isolated from the  
297 fruit clusters of *P. vulgaris* with spherical conformation, exhibited significant  
298 immunomodulatory activities *in vitro*. Further research is required to demonstrate that P1 can

299 impact macrophages *in vivo*.

300 *3.4.2. Effects of Anti-TLR2, Anti-TLR4, Anti-CR3 and Dectin-1 Treatments on P1-induced*  
301 *Cytokine production*

302 Activated macrophage can kill tumor cells and pathogens by either direct killing or releasing  
303 diffusible cytokines. It is thought to be mediated through the recognition of polysaccharide by  
304 specific immune receptors.<sup>4</sup> Studies suggested that polysaccharides could mediate  
305 immunomodulatory effects through the TLR2, TLR4, CR3, or Dectin-1 membrane receptors.<sup>18,</sup>  
306 <sup>19, 42</sup> To further determine the membrane receptor of P1, RAW 246.7 cells were treated with  
307 anti-TLR2, anti-TLR4, anti-CR3 antibodies or the Dectin-1 inhibitor Lam for 1 h before  
308 stimulation of P1. Lam, a soluble  $\beta$ -glucan, was reported as the inhibitor of Dectin-1 activity  
309 through binding to Dectin-1.<sup>43</sup> Then Lam was employed to further study the potential role of  
310 Dectin-1.<sup>18</sup> The production of NO, TNF- $\alpha$ , and IL-6 in RAW 246.7 cells was measured. As  
311 shown in Fig. 8a, treatment of RAW 246.7 cells with anti-TLR2 reduced the P1-induced NO  
312 production by 64%. However, the anti-TLR4, anti-CR3, and Lam were unable to inhibit the  
313 secretion of NO. The results suggested that P1 induced NO production through the activation of  
314 TLR2. As shown in Fig. 8c, after anti-TLR2, anti-TLR4, and anti-CR3 incubation, the  
315 production of IL-6 was decreased by 42, 37, and 38%, respectively, but still significantly higher  
316 than that in the absence of P1 stimulation. The Lam did not inhibit the increase in IL-6  
317 production. The results suggested that P1 induced IL-6 production through the activation of  
318 TLR2, TLR4, and CR3. However, no reduced TNF- $\alpha$  production was observed after the  
319 treatment with four antibodies, indicating different signaling pathways for NO, TNF- $\alpha$ , and  
320 IL-6 production in RAW 246.7 cells (Fig. 8b). Other immune membrane receptors may also be

321 possible.

322 The TLR signaling pathways generally include two distinct pathways depending on the  
323 adaptor molecules, myeloid differentiation factor 88 (MyD88) and TIR domain-containing  
324 adaptor inducing interferon- $\beta$  (TRIF). TLR2 and TLR4 trigger MyD88 signaling, which  
325 activates mitogen-activated protein (MAP) kinase and nuclear factor (NF)- $\kappa$ B to induce  
326 expression of proinflammatory cytokines genes. TLR4 also activates TRIF-dependent signaling,  
327 which activates interferon regulatory factor 3 (IRF3) to induce the expression of  
328 proinflammatory cytokines genes and type 1 IRF3.<sup>2</sup> CR3 activates spleen tyrosine kinase (syk)  
329 signaling, which activates NF- $\kappa$ B to induce expression of proinflammatory cytokines genes.<sup>44</sup>  
330 Han et al. (2009a) demonstrated that an aqueous extract of *P. vulgaris* could stimulate  
331 macrophage activation via NF- $\kappa$ B transactivation and MAP kinase activation.<sup>9</sup> Therefore, we  
332 deduced that P1 might activate macrophage to release the above mediators partly involving the  
333 NF- $\kappa$ B signaling pathway. The results might provide references to the signal transduction and  
334 molecular mechanisms of P1-induced macrophage activation.

#### 335 3.4.3. Effects of P1 on Cytokine Production under Different pH and Thermal Treatments

336 Thermal and different environmental condition treatments can change the structure of  
337 polysaccharide and cause the loss of activity.<sup>19, 45</sup> Effects of thermal and different pH treatments  
338 on the activity of P1 were investigated. As shown in Fig. 9a, there were no obvious changes in  
339 NO, TNF- $\alpha$ , and IL-6 production in RAW 246.7 cells induced by P1 treated with temperatures  
340 below 121 °C. However, after high-temperature treatment at 145 °C for 20 min, P1 almost lost  
341 all of its secretion-inducing ability of NO, TNF- $\alpha$ , and IL-6. Previous studies showed that the  
342 ordered conformation of polysaccharide could be disrupted by thermal treatment at about

343 137-145 °C.<sup>45</sup> However, the chemical bonds could not be changed.<sup>19</sup> The GPC analysis also  
344 demonstrated that there was no difference in the molecular weight between thermal treated and  
345 untreated P1, indicating the chemical bonds of P1 were not broken. The result indicated that the  
346 ordered conformation of P1 was changed by thermal treatment at 145 °C, resulting in the loss  
347 of immune activity. As shown in Fig. 9b, after treatment for 12 h at solutions ranging from pH  
348 2.0 to 10.0, P1 maintained active conformation and was also able to induce the secretion of NO,  
349 TNF- $\alpha$ , and IL-6. However, after treatment with pH 2.0 solvent, P1 almost lose all of its activity,  
350 with the NO, TNF- $\alpha$ , and IL-6 production equal to the control groups (without P1). These  
351 results showed that P1 had high stability in the pH range of 4.0 to 10.0. Therefore, P1 has the  
352 potential of being used as a immunomodulatory agent in the drug and food industries.

#### 353 4. Conclusion

354 In this study, a new heteropolysaccharide P1 was isolated from *P. vulgaris* using boiling  
355 water. P1 had an average molecular weight of 1,750 kDa and was composed of Ara, Xyl, Man,  
356 Glu, and Gal with molar percentages of 28.37, 54.67, 5.61, 5.46, and 5.89%, respectively. AFM  
357 analysis showed that P1 had a spherical conformation when dispersed in water. P1 showed  
358 significant immuno-stimulating activities involving TLR2, TLR4 and CR3. P1 exhibited highly  
359 stable immuno-stimulating activities in the pH range of 4.0-10.0 and below 121 °C. Our results  
360 demonstrated that P1 could be used as a potential complementary medicine or functional food.  
361 In-depth studies on the immunomodulatory activity *in vivo* and molecular mechanisms of action  
362 of P1 are in progress.

#### 363 Conflicts of interest

364 The authors have no conflict of interest to declare.

365 **Acknowledgments**

366 We gratefully acknowledge the financial support from the Guangzhou Science and  
367 Technology Program (2013J4500036), the Guangdong Science and Technology Program  
368 (2012B050500003), the Program for Leading Talent of Guangdong Province (Rui Hai Liu) and  
369 the State Scholarship Fund provided by China Scholarship Council for Chao Li. The critical  
370 review and editing of the manuscript by Professor Qingrong Huang at Rutgers University is  
371 most appreciated.

372 **References**

- 373 1. A. Klimp, E. De Vries, G. Scherphof and T. Daemen, *Crit Rev Oncol Hemat*, 2002, 44,  
374 143-161.
- 375 2. O. Takeuchi and S. Akira, *Cell*, 2010, 140, 805-820.
- 376 3. I. A. Schepetkin and M. T. Quinn, *Int Immunopharmacol*, 2006, 6, 317-333.
- 377 4. J. L. Stow, P. C. Low, C. Offenhauser and D. Sangermani, *Immunobiology*, 2009, 214,  
378 601-612.
- 379 5. S. J. Wu, C. C. Liaw, S. Z. Pan, H. C. Yang and L. T. Ng, *J Funct Foods*, 2013, 5,  
380 679-688.
- 381 6. G.-H. Wu, C.-L. Lu, J.-G. Jiang, Z.-Y. Li and Z.-L. Huang, *Food Funct*, 2014, 5,  
382 337-344.
- 383 7. Y. Zhang, S. Li, X. Wang, L. Zhang and P. C. K. Cheung, *Food Hydrocolloid*, 2011, 25,  
384 196-206.
- 385 8. C. Li, X. Fu, Q. Huang, F. Luo and L. You, *Eur Food Res Technol*, 2015, 240, 49-60.
- 386 9. E. H. Han, J. H. Choi, Y. P. Hwang, H. J. Park, C. Y. Choi, Y. C. Chung, J. K. Seo and H.

- 387 G. Jeong, *Food Chem Toxicol*, 2009, 47, 62-69.
- 388 10. H. Y. Cheung and Q. F. Zhang, *J Chromatogr A*, 2008, 1213, 231-238.
- 389 11. X. Fang, M. M.-S. Yu, W.-H. Yuen, S. Y. Zee and R. C.-C. Chang, *Int J Mol Med*, 2005,  
390 16, 1109-1116.
- 391 12. S.-Y. Kim, S.-H. Kim, H.-Y. Shin, J.-P. Lim, B.-S. Chae, J.-S. Park, S.-G. Hong, M.-S.  
392 Kim, D.-G. Jo and W.-H. Park, *Exp Biol Med*, 2007, 232, 921-926.
- 393 13. C. Li, Q. Huang, X. Fu, X.-J. Yue, R. H. Liu and L.-J. You, *Int J Biol Macromol*, 2015,  
394 75, 298-305.
- 395 14. M. Dubois, K. A. Gilles, J. K. Hamilton, P. A. Rebers and F. Smith, *Anal Chem*, 1956,  
396 28, 350-356.
- 397 15. C. Li, X. Fu, F. Luo and Q. Huang, *Food Hydrocolloid*, 2013, 32, 79-86.
- 398 16. L. You, Q. Gao, M. Feng, B. Yang, J. Ren, L. Gu, C. Cui and M. Zhao, *Food Chem*,  
399 2013, 138, 2242-2249.
- 400 17. Z.-M. Wang, X. Peng, K.-L. D. Lee, J. C.-o. Tang, P. C.-K. Cheung and J.-Y. Wu, *Food*  
401 *Chem*, 2011, 125, 637-643.
- 402 18. Y. Wang, J. Fang, X. Ni, J. Li, Q. Liu, Q. Dong, J. Duan and K. Ding, *J Agr Food Chem*,  
403 2013, 61, 11400-11409.
- 404 19. X. Xu, H. Yan and X. Zhang, *J Agr Food Chem*, 2012, 60, 11560-11566.
- 405 20. Y. Jing, L. Huang, W. Lv, H. Tong, L. Song, X. Hu and R. Yu, *J Agric Food Chem*, 2014,  
406 62, 902-911.
- 407 21. C. Liu, Q. Lin, Y. Gao, L. Ye, Y. Xing and T. Xi, *Carbohydr Polym*, 2007, 67, 313-318.
- 408 22. F. Tao, G. Zheng Biao, J. Zheng Yu and Z. Hai Ning, *Carbohydr Polym*, 2008, 71,

- 409 159-169.
- 410 23. J. Zhu, W. Liu, J. Yu, S. Zou, J. Wang, W. Yao and X. Gao, *Carbohydr Polym*, 2013, 98,  
411 8-16.
- 412 24. M. Ghasemlou, F. Khodaiyan, K. Jahanbin, S. M. T. Gharibzahedi and S. Taheri, *Food*  
413 *Chem*, 2012, 133, 383-389.
- 414 25. C. Liu, X. Li, Y. Li, Y. Feng, S. Zhou and F. Wang, *Food Chem*, 2008, 110, 807-813.
- 415 26. C. Yan, Y. Yin, D. Zhang, W. Yang and R. Yu, *Carbohydr Polym*, 2013, 96, 389-395.
- 416 27. L. Feng, X. Jia, F. Shi and Y. Chen, *Molecules*, 2010, 15, 5093-5103.
- 417 28. Y. B. Xi, Y. F. Wu and G. Chen, *Journal of Guangdong Pharmaceutical College*, 2010,  
418 26, 594-598.
- 419 29. G. H. Wu, T. Hu, Z. L. Huang and J. G. Jiang, *Carbohydr Polym*, 2013, 96, 284-290.
- 420 30. O. H. Willemsen, M. M. Snel, A. Cambi, J. Greve, B. G. De Grooth and C. G. Figdor,  
421 *Biophys J*, 2000, 79, 3267-3281.
- 422 31. L. Chen, W. Xu, S. Lin and P. C. K. Cheung, *Food Hydrocolloid*, 2014, 36, 189-195.
- 423 32. Z. H. Liu, Y. P. Jiao, Y. F. Wang, C. R. Zhou and Z. Y. Zhang, *Adv Drug Delivery Rev*,  
424 2008, 60, 1650-1662.
- 425 33. P. Hwang, S. Chien, Y. Chan, M. Lu, C. Wu, Z. Kong and C. Wu, *J Agr Food Chem*,  
426 2011, 59, 2062-2068.
- 427 34. G. Karupiah, Q.-w. Xie, R. Buller, C. Nathan, C. Duarte and J. D. MacMicking, *Science*,  
428 1993, 261, 1445-1448.
- 429 35. I. B. Jeff, X. Yuan, L. Sun, R. M. Kassim, A. D. Foday and Y. Zhou, *Int J Biol*  
430 *Macromol*, 2013, 52, 99-106.

- 431 36. V. Vetvicka and J.-C. Yvin, *Int Immunopharmacol*, 2004, 4, 721-730.
- 432 37. B. H. Falch, T. Espevik, L. Ryan and B. T. Stokke, *Carbohyd Res*, 2000, 329, 587-596.
- 433 38. U. Surenjav, L. Zhang, X. Xu, X. Zhang and F. Zeng, *Carbohydr Polym*, 2006, 63,  
434 97-104.
- 435 39. L. Zhang, X. Li, X. Xu and F. Zeng, *Carbohyd Res*, 2005, 340, 1515-1521.
- 436 40. X. Xu, H. Yan and X. Zhang, *J Agr Food Chem*, 2012, 60, 11560-11566.
- 437 41. Y. Tao, L. Zhang and P. C. Cheung, *Carbohyd Res*, 2006, 341, 2261-2269.
- 438 42. S. Chen, D. K. Yin, W. B. Yao, Y. D. Wang, Y. R. Zhang and X. D. Gao, *Acta Pharmacol*  
439 *Sin*, 2009, 30, 1008-1014.
- 440 43. B. N. Gantner, R. M. Simmons, S. J. Canavera, S. Akira and D. M. Underhill, *J Exp*  
441 *Med*, 2003, 197, 1107-1117.
- 442 44. G. C. Chan, W. K. Chan and D. M. Sze, *J Hematol Oncol*, 2009, 2, 25-35.
- 443 45. X. Wang, X. Xu and L. Zhang, *J Phys Chem B*, 2008, 112, 10343-10351.
- 444

445 **Figure Captions**

446 **Fig. 1** Chromatogram of P1 by Sephadex G-100 (A) and GPC (B)

447 **Fig. 2** IR spectrum of P1 (A), standard curve of galacturonic acid (B) and ion chromatography of  
448 galacturonic acid in P1 (C)

449 **Fig. 3** Gas chromatography (GC) results of acetyl derivatives of monosaccharide standards (A)  
450 and hydrolyzate of P1 (B).

451 **Fig. 4** Gas chromatography (GC) results of acetyl derivatives of standards (A), Smith  
452 degradation product of P1 (B) and the standard curve of NaIO<sub>4</sub> (C).

453 **Fig. 5** NMR spectra of the polysaccharide P1 in D<sub>2</sub>O: (A) <sup>1</sup>H NMR and (B) <sup>13</sup>C NMR.

454 **Fig. 6** The AFM (scale: 3.0 μm × 3.0 μm) image height of P1 in distilled water.

455 **Fig. 7** Effects of the different concentrations of P1 on production of NO (A), TNF-α (B), and  
456 IL-6 (C) in RAW 264.7 cells. Lipopolysaccharides (LPS, 50 μg/mL) were used as the positive  
457 control. Bars with no letter in common are significantly different ( $p < 0.05$ ).

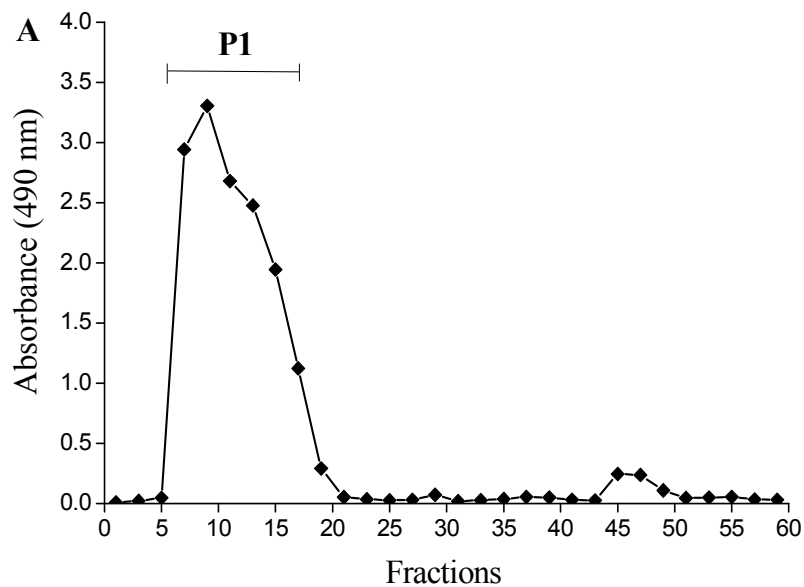
458 **Fig. 8** Effects of anti-TLR2 (aTLR2), anti-TLR4 (aTLR4), anti-CR3 (aCR3), and Dectin-1  
459 treatments on P1-induced NO (A), TNF-α (B), and IL-6 (C) production in RAW 264.7 cells.  
460 Laminarin (Lam) was used as the Dectin-1 inhibitor. The cells were incubated with monoclonal  
461 antibodies for 1 h and then washed extensively before stimulation with P1 (250 μg/mL). <sup>a</sup> $p <$   
462 0.05 versus the P1 group.

463 **Fig. 9a** Effects of different temperature on P1-induced NO (A), TNF-α (B), and IL-6 (C)  
464 production in RAW 264.7 cells. The cells were incubated with P1 (400 μg/mL) for 24 h. The P1  
465 was treated at different temperature. <sup>a</sup> $p < 0.05$  versus the untreated group.

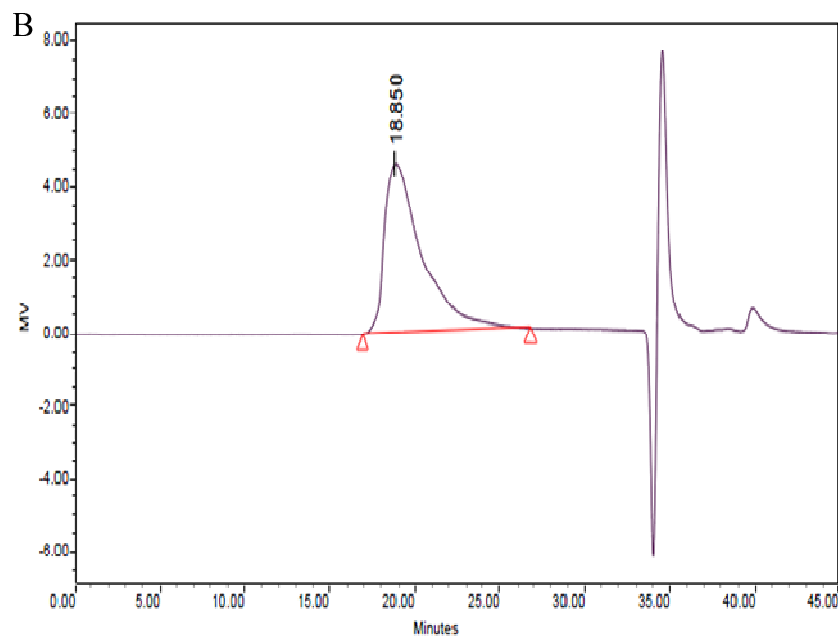
466 **Fig. 9b** Effects of different pH on P1-induced NO (A), TNF-α (B), and IL-6 (C) production in

467 RAW 264.7 cells. The cells were incubated with P1 (400 µg/mL) for 24 h. The P1 was treated at  
468 PBS of different pH. <sup>a</sup> $p < 0.05$  versus the untreated group.

469 Fig. 1

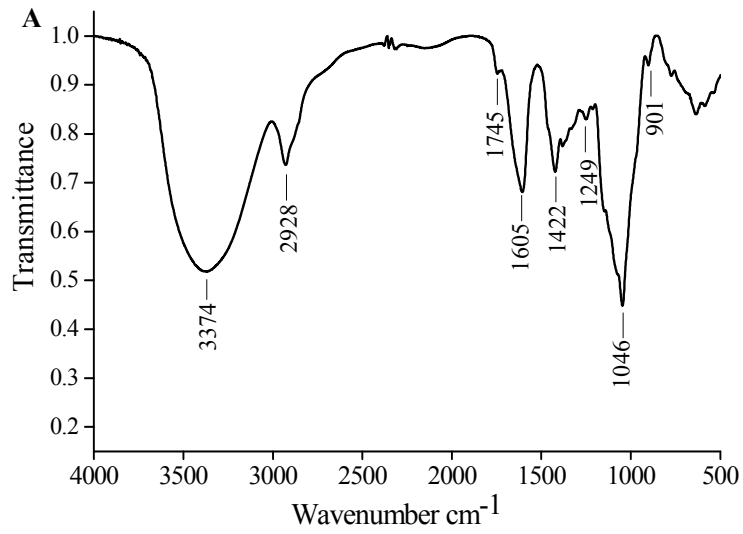


470

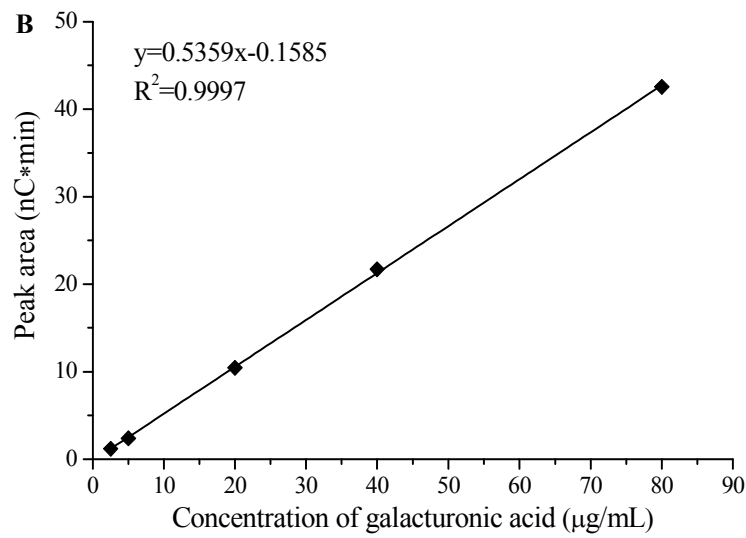


471

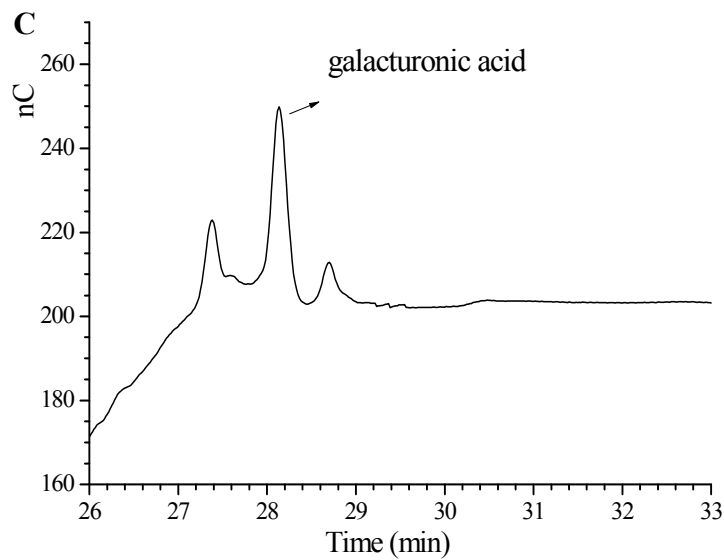
472 Fig. 2



473

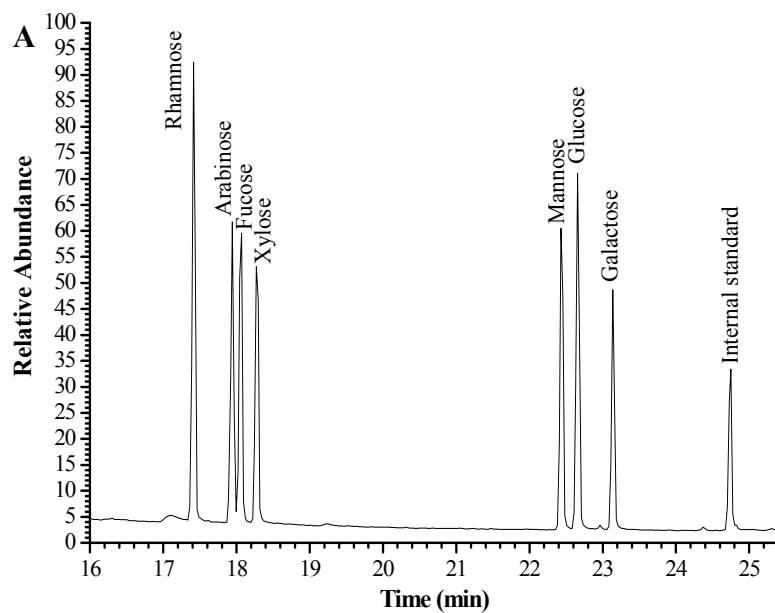


474

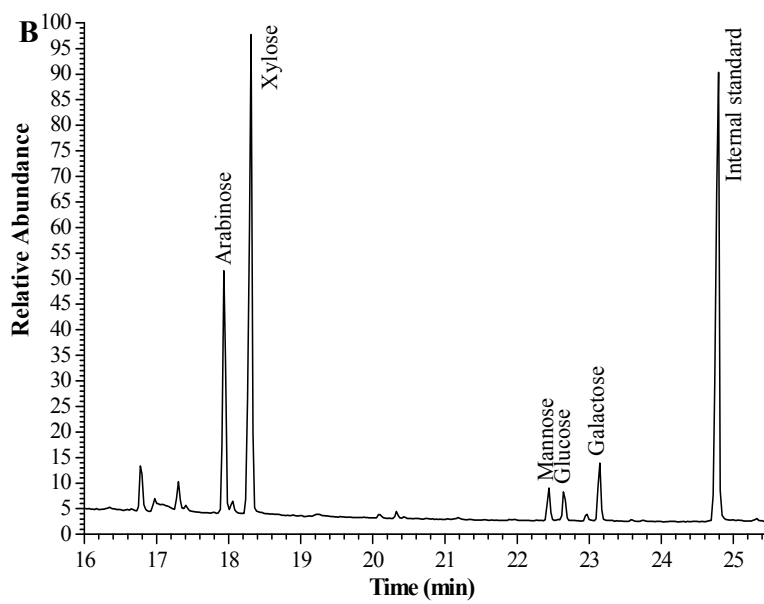


475

476 Fig. 3

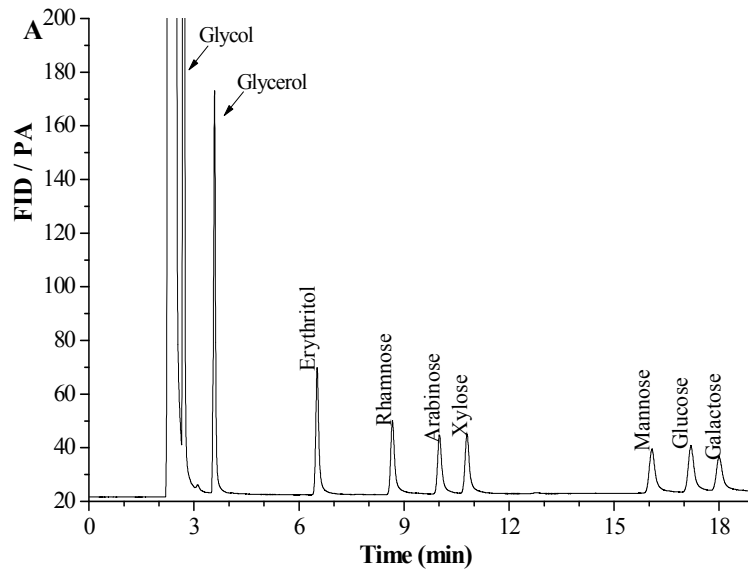


477

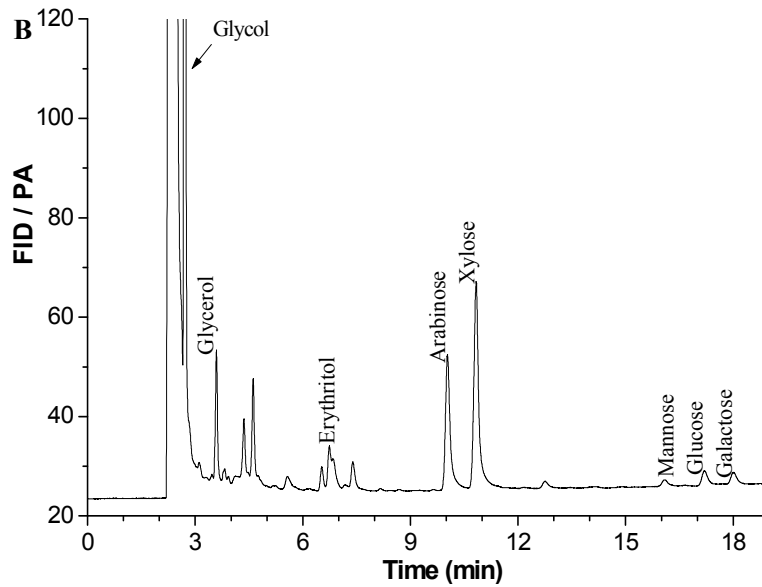


478

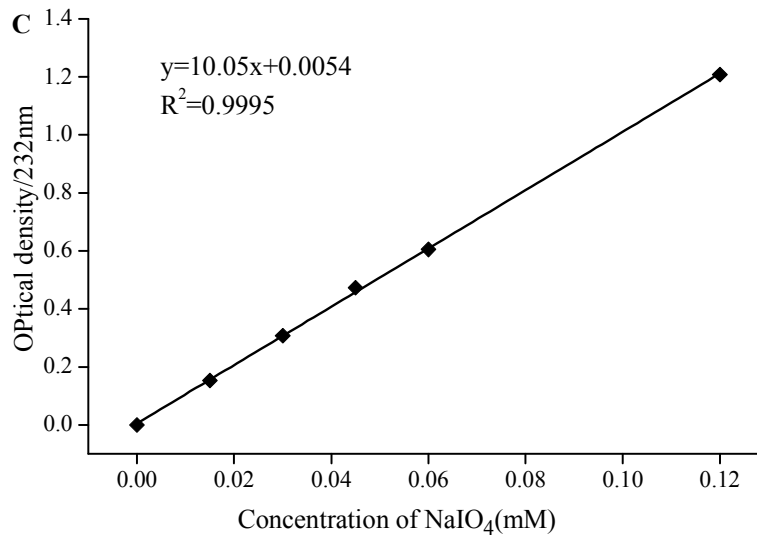
479 Fig. 4



480

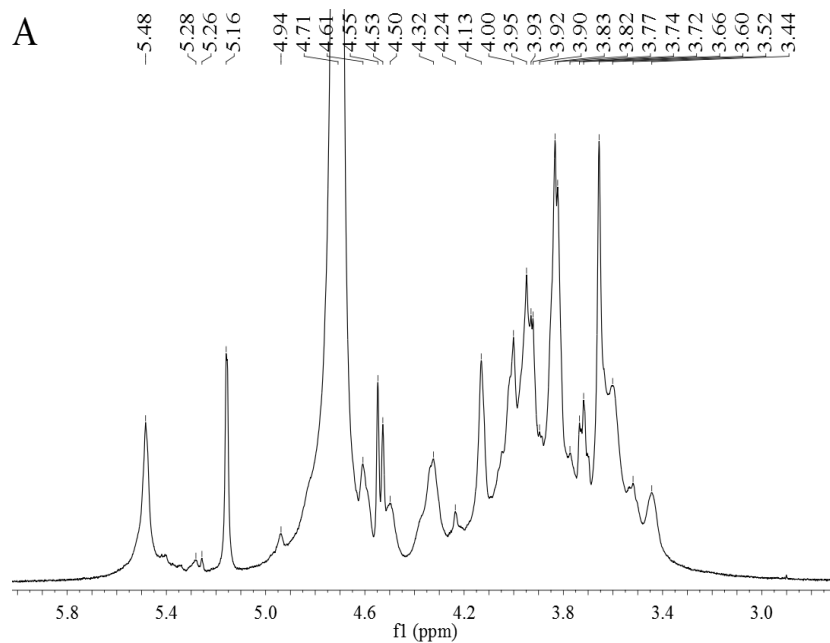


481

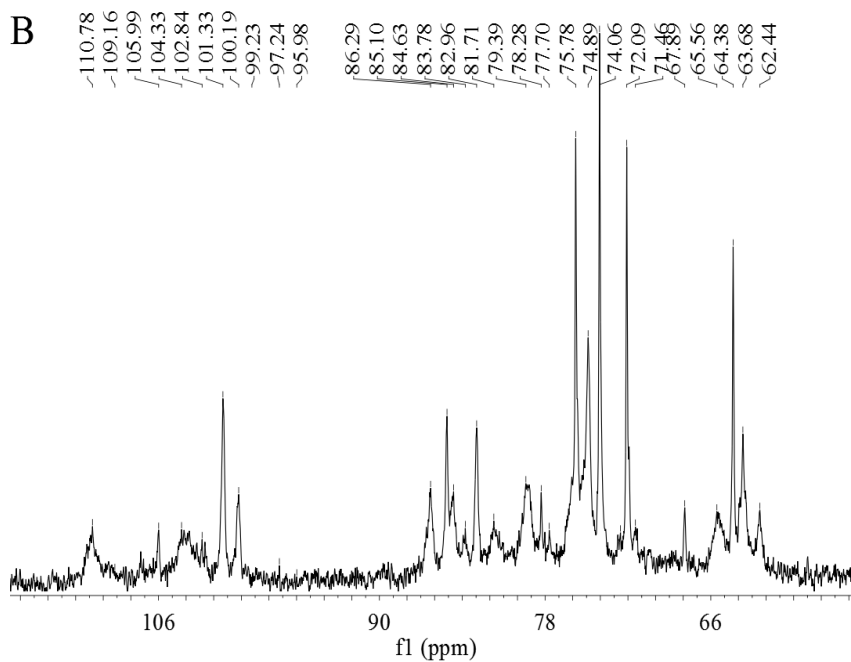


482

483 Fig. 5



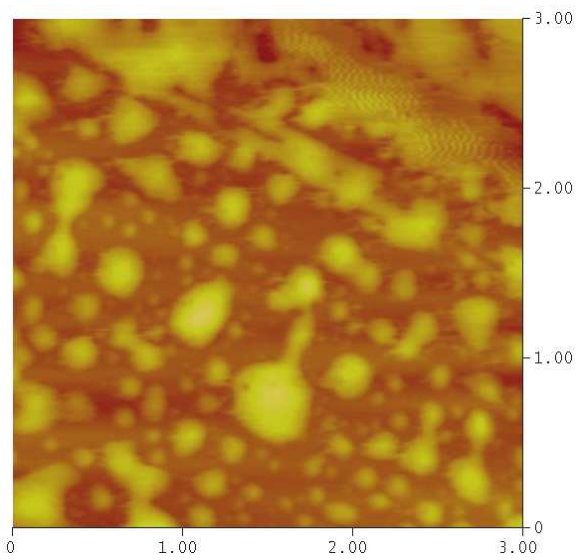
484



485

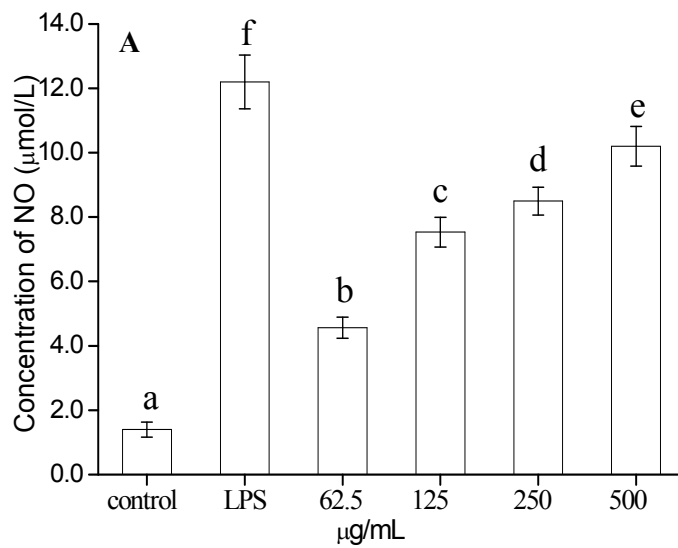
486

487 **Fig. 6**

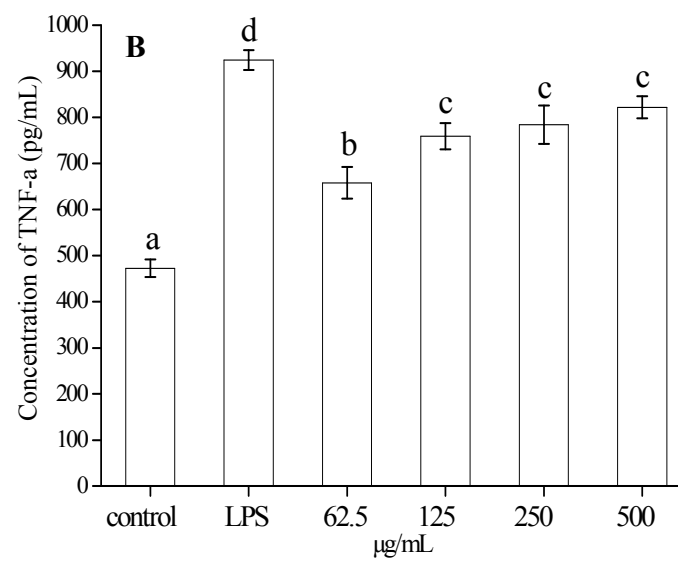


488

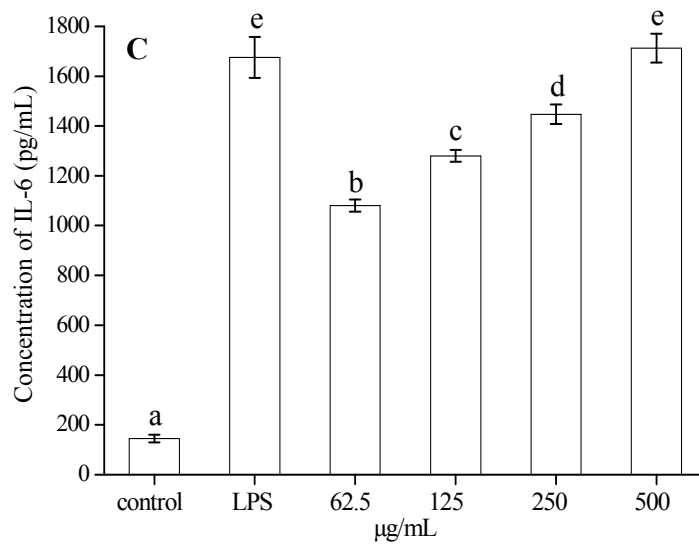
489 Fig. 7



490



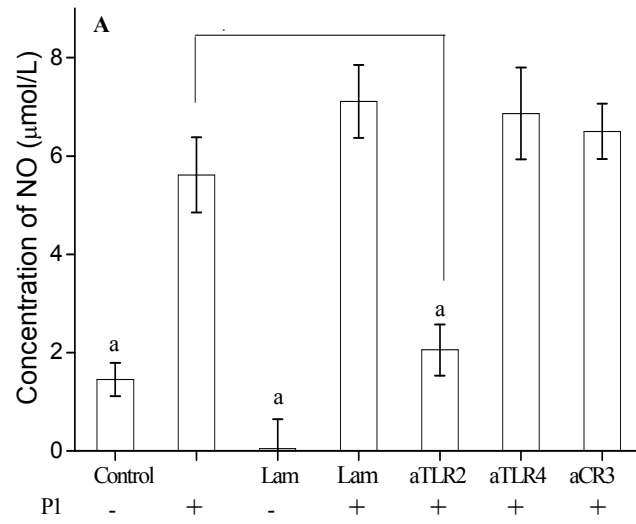
491



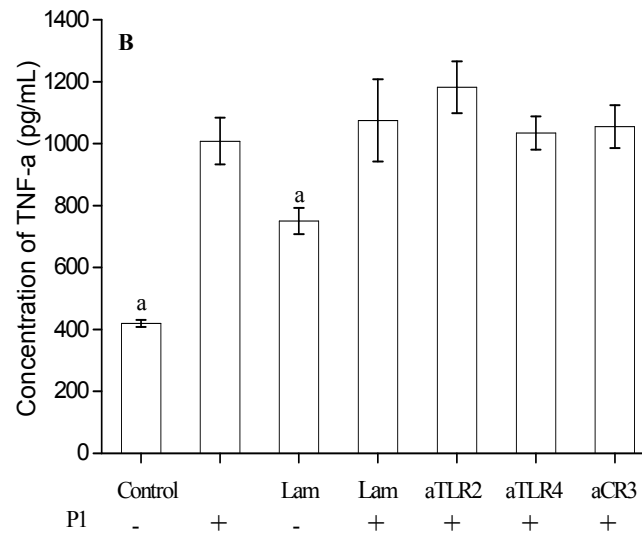
492

493 Fig. 8

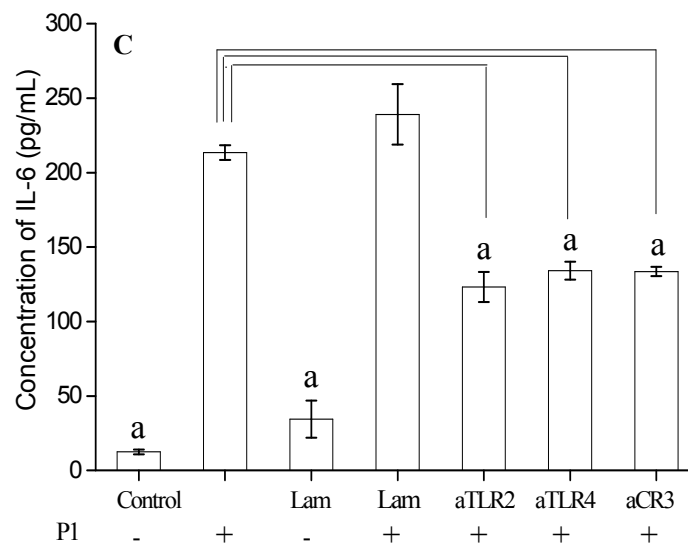
494



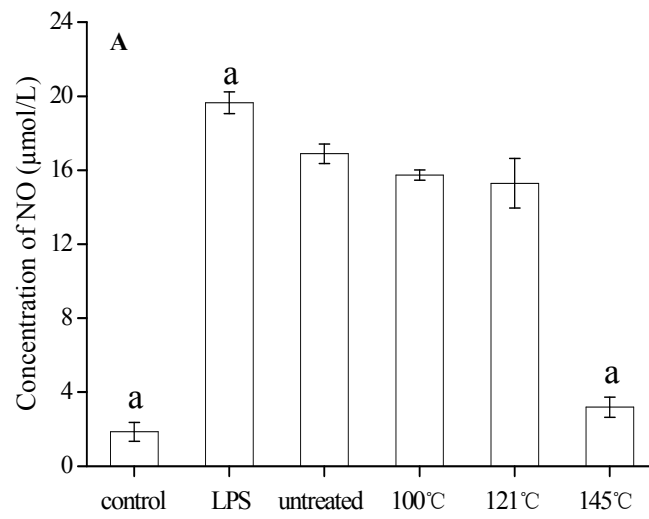
495



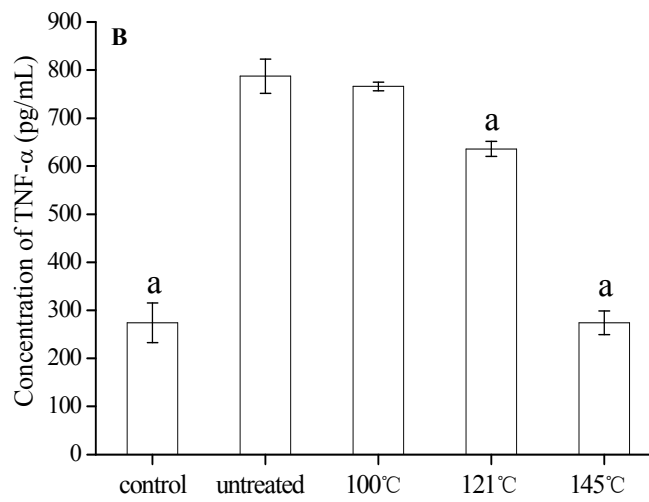
496



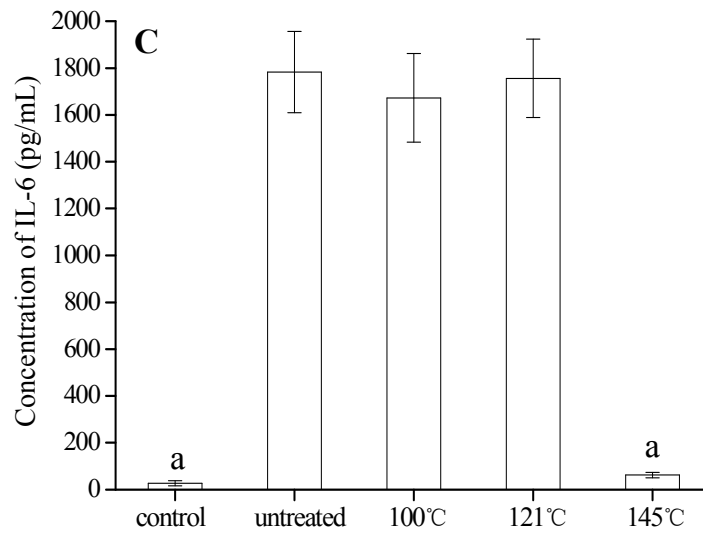
497 Fig. 9a



498



499



500

501 Fig. 9b

